 

PACS numbers: 42.55.Px; 42.55.Xi; 42.60.Jf
DOI: 10.1070/QE2005v035n12ABEH013037

# Spatial radiation intensity distribution of linear diode arrays and calculation of inversion in fibre-coupled end-pumped solid-state lasers

M.V. Gorbunkov, P.V. Kostryukov, V.B. Morozov, A.N. Olenin, L.S. Telegin, V.G. Tunkin, D.V. Yakovlev

***Abstract*. The radiation intensity distribution of linear diode arrays used for longitudinal pumping fibre-coupled solid-state lasers is studied experimentally and theoretically. A simple model describing the propagation of radiation is proposed which allows the calculation of the inversion population distribution in an active element. The radiation intensity distributions are calculated in cross sections for different angular distributions at the fibre output.**

***Keywords***: *diode pumping, optical fibres, solid-state lasers.*

Diode pumping of solid-state lasers is finding increasing use due to its high efficiency. The efficiency (light – light) of lasing at several transverse modes can be as high as 70 % [1, 2]. For many applications, single-mode lasing is preferable. Thus, highly efficient (58 %) single-mode lasing with nearly $TEM_{00}$ mode field distribution obtained upon transverse pumping (without an optical fibre) was reported in [3]. The spatial inhomogeneity of pump radiation was averaged by means of a rather intricate scheme involving total internal reflection in an active element and a specially developed astigmatism-corrected resonator with cylindrical elements. Another, and possibly simpler method for efficient generation of single-mode radiation, is longitudinal pumping. High-power pumping is provided by diode bars and arrays. The radiation of diode arrays is delivered, as a rule, by means of multimode fibres of diameter 0.2 – 0.8 mm [4 – 6]. Although linear diode arrays with a fibre pigtail are widespread, no experimental data are available in the literature about the spatial radiation distribution upon longitudinal pumping, and simulations of this distribution and calculations of the real inversion distribution in the active element have not been described.

At the same time, to match optimally the spatial distribution of the pump radiation with a laser mode, the method using simplified spatial intensity distributions (rectangular, Gaussian or super-Gaussian) of the pump radiation in different cross sections of an active element is often employed [7 – 11]. Radiation transferred through fibres noticeably differs from coherent radiation used upon conventional pumping. During its transfer to an active element, a number of substantial features appear in the spatial intensity distribution. The use of simplified spatial distributions does not allow the matching of the pump radiation with a laser mode for increasing the lasing efficiency by preserving the acceptable quality of the output radiation.

This paper is devoted to simulation of the spatial distribution of inversion produced by radiation from linear diode arrays in fibre-coupled end-pumped solid-state lasers. We analysed in detail the spatial distribution of the pump radiation near the image plane of the fibre end. The results of our calculations allow us to formulate the strategy for optimal matching of the pump radiation with the output radiation field for real experimental conditions.

In [6], we performed the longitudinal pumping of a repetitively pulsed picosecond Nd:YAG laser by an JOLD-35 linear diode array with a pigtail emitting 35-W, 300-μs pulses. The fibre diameter was 0.8 mm. The unexpectedly large variations in the lasing threshold were observed when the conditions of radiation transport in the fibre were changed (by fibre bending or twisting). The sensitivity to the active-element displacement along the pump axis was a few millimetres. To explain these features, it is necessary to study in detail the spatial radiation intensity distribution of diode arrays with a pigtail.

An important function of a fibre is the spatial and angular averaging of individual diodes comprising a diode array. It is known that, to obtain a nearly rectangular spatial radiation distribution at the diode array output, fibres of length from a few tens to hundreds metres coiled in rings in two perpendicular planes are required. Commercial diode arrays are equipped with considerably shorter fibres. With such fibres, the degree of parameter averaging and the spatially-angular radiation distribution considerably depend on the fibre bending.

Upon transfer of the pump radiation in a perfect optical system, there exists a separated plane – the image plane of the fibre end. The radiation distribution in this plane is independent of the angular radiation distribution at the fibre output. If the spatial radiation distribution over the fibre end is rectangular, the radiation intensity distribution in the image plane will be also rectangular. It is not at all obvious that the rectangular distribution is optimal for spatial matching with a Gaussian mode. It is not inconceivable that preferable is the intensity distribution obtained upon

**M.V. Gorbunkov** P.N. Lebedev Physics Institute, Russian Academy of Sciences, Leninskii prosp. 53, 119991 Moscow, Russia;
e-mail: gorbunkov@sci.lebedev.ru;
**P.V. Kostryukov, V.B. Morozov, A.N. Olenin, L.S. Telegin, V.G. Tunkin, D.V. Yakovlev** International Laser Center, M.V. Lomonosov Moscow State University, Vorob'evy gory, 119992 Moscow, Russia;
e-mail: vgtunkin@mail.ru

Received 21 June 2005; revision received 2 September 2005
*Kvantovaya Elektronika* **35** (12) 1121 – 1125 (2005)
Translated by M.N. Sapozhnikov

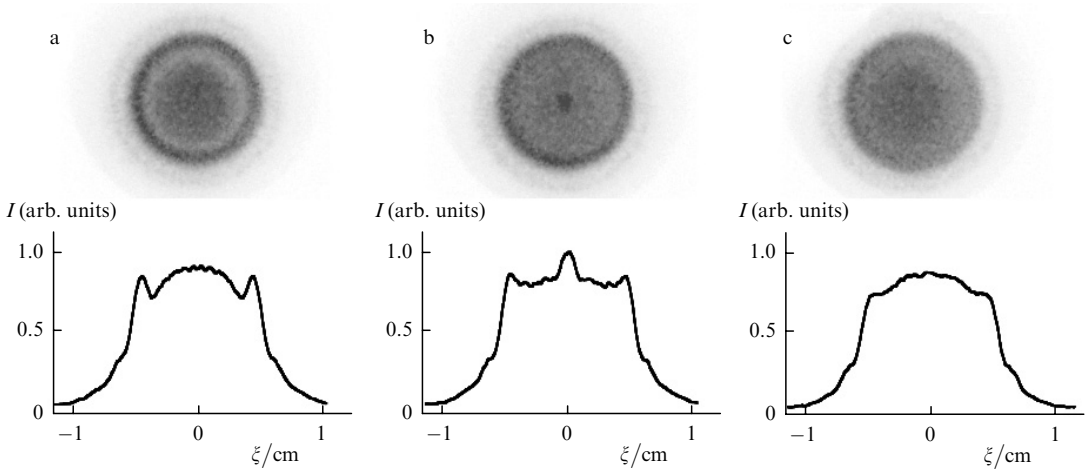


**Figure 1.** Angular radiation intensity distributions at the output of a fibre of length 55 cm observed after the radiation transport through the linear (a), bent (b), and bent and twisted (c) fibre. The corresponding intensity profiles are also shown, as in Figs 2 and 5.

some displacement from the image plane due to a soft aperture caused by the inhomogeneous distribution of the gain in the active medium. It is important that the intensity distribution outside the image plane depends on the angular radiation distribution at the fibre output. Therefore, we studied first the stability and reproducibility of the angular distribution of pump radiation propagating in multimode fibres of different lengths.

Figure 1 shows the output angular intensity distributions for a fibre of length 55 cm and diameter 0.8 mm for different conditions of radiation transport in the fibre. These distributions were obtained by photographing the intensity distribution on a ground glass located in the focal plane of a wide-aperture ERA 4-T objective. The intensity distribution pattern depends on the radiation transport conditions. Thus, the distribution most close to a uniform one is achieved only if a bent and twisted fibre is used. Further experiments were performed with a fibre of diameter 0.8 mm and length 3.9 m, which was coiled to several rings. We obtained the transport conditions providing the sufficient uniformity and reproducibility of the spatially-angular radiation distribution. Figure 2 shows the image of the fibre end obtained with an ERA 4-T objective and the angular radiation distribution obtained in the focal plane of the same objective. The radiation distribution over the fibre end is close to the rectangular one and the angular distribution is close to a Gaussian.

We simulated the propagation of an incoherent pump beam emerging from a fibre and focused by a lens to the active medium and calculated the inverse population distribution in the active medium by the method close to that considered in [12]. This model can be easily experimentally verified by measuring the transverse radiation intensity distribution in different planes. The spatial position of a point is specified by the Cartesian coordinates and the beam direction is specified by the angles $\alpha$ and $\gamma$. The angle $\gamma$ is formed by the beam itself and the optical axis of the system along which the coordinate axis $z$ is directed, while the angle $\alpha$ is formed by the beam projection on the $xy$ plane and the ordinate axis, and $0 \leqslant \alpha < 2\pi$ and $0 \leqslant \gamma < \pi/2$ (Fig. 3).

If the region $0 \leqslant z \leqslant L$ is filled with a medium with the refractive index $n$, the output parameters $[x_2 = x(z = L)$, $y_2 = y(z = L)$, $\alpha_2 = \alpha(z = L + 0)$ and $\gamma_2 = \gamma(z = L + 0)]$ can be calculated from the specified parameters $[x_1 = x(z = 0)$, $y_1 = y(z = 0)$, $\alpha_1 = \alpha(z = -0)$ and $\gamma_1 = \gamma(z = -0)]$ at the input $(z = -0)$:

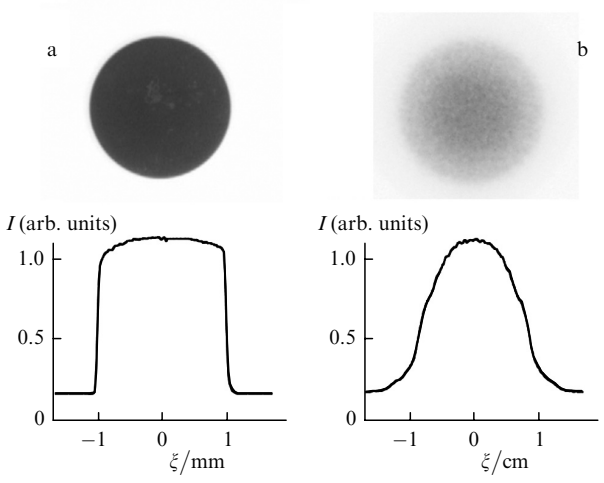


**Figure 2.** Intensity distributions in the end image plane of a fibre of length 3.9 m (a) and in the objective focal plane (b).

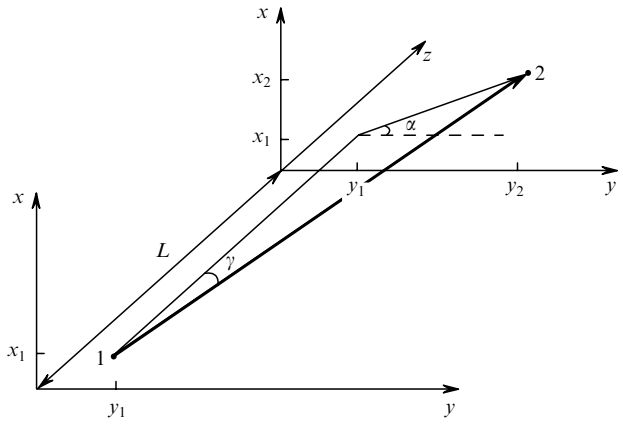


**Figure 3.** Spatial position of a beam and coordinates used for its description; 1 and 2 are the points of beam input in and output from a medium.

$$x_2 = x_1 + \frac{\gamma_1}{n} L \sin\alpha_1,$$

$$y_2 = y_1 + \frac{\gamma_1}{n} L \cos\alpha_1, \qquad (1)$$

$$\gamma_2 = \gamma_1,$$

$$\alpha_2 = \alpha_1.$$

In the case of a thin lens with the focal length $f$ located in the plane $z = 0$, the parameters $\alpha_1 = \alpha(z = -0), \gamma_1 = \gamma(z = -0), \alpha_2 = \alpha(z = +0)$ and $\gamma_2 = \gamma(z = +0)$ are described by the expressions

$$x_2 = x_1,$$

$$y_2 = y_1, \qquad (2)$$

$$\gamma_2 = \frac{[(y_1 - \gamma_1 f\cos\alpha_1)^2 + (x_1 - \gamma_1 f\sin\alpha_1)^2]^{1/2}}{f},$$

$$\alpha_2 = \arg[(y_1 - \gamma_1 f\cos\alpha_1) + \mathrm{i}(x_1 - \gamma_1 f\sin\alpha_1)],$$

where $\arg(x + \mathrm{i}y)$ corresponds to the value of the polar angle $\varphi \in [0, 2\pi)$ in the coordinate system $\rho, \varphi$, for a point with the Cartesian coordinates $x$, $y$.

The above relations allow the calculation of the trajectory of each of the beams and, correspondingly, the intensity distribution from the known initial parameters $x$, $y$, $\alpha$, and $\gamma$ of the beam in the input plane $z = 0$.

It was assumed in the calculation that the lens is thin and the fibre end consists of a set of independent sources emitting beams with the specified angular distribution. It was also assumed that the radiation intensity at a point in an empty space is proportional to the number of beams passing through a surface element. The pump radiation intensity distribution in the absorbing active medium was calculated by taking into account energy losses along the beam propagation direction. Because the population inversion in a four-level system is proportional to the absorbed power, the intensity distribution in the active medium, calculated taking absorption into account, coincides with the inversion distribution with an accuracy to a coefficient.

The calculation was performed for a lens with the focal length 15 mm for the transfer of the fibre end image at the 1 : 1 scale. The intensity distributions in different planes near the image plane were calculated for the rectangular intensity distribution over the fibre end and different angular distributions. The total number of beams emerging from the fibre was the same for all the angular distributions. Figure 4 shows the radiation intensity distributions calculated in the vicinity of the image plane.

The intensity distribution in the image plane of the fibre end is shown in Fig. 4g. As expected, in this case the intensity distribution is independent of the angular distribution. Noticeable differences between spatial distributions appear upon displacement from the image plane by a

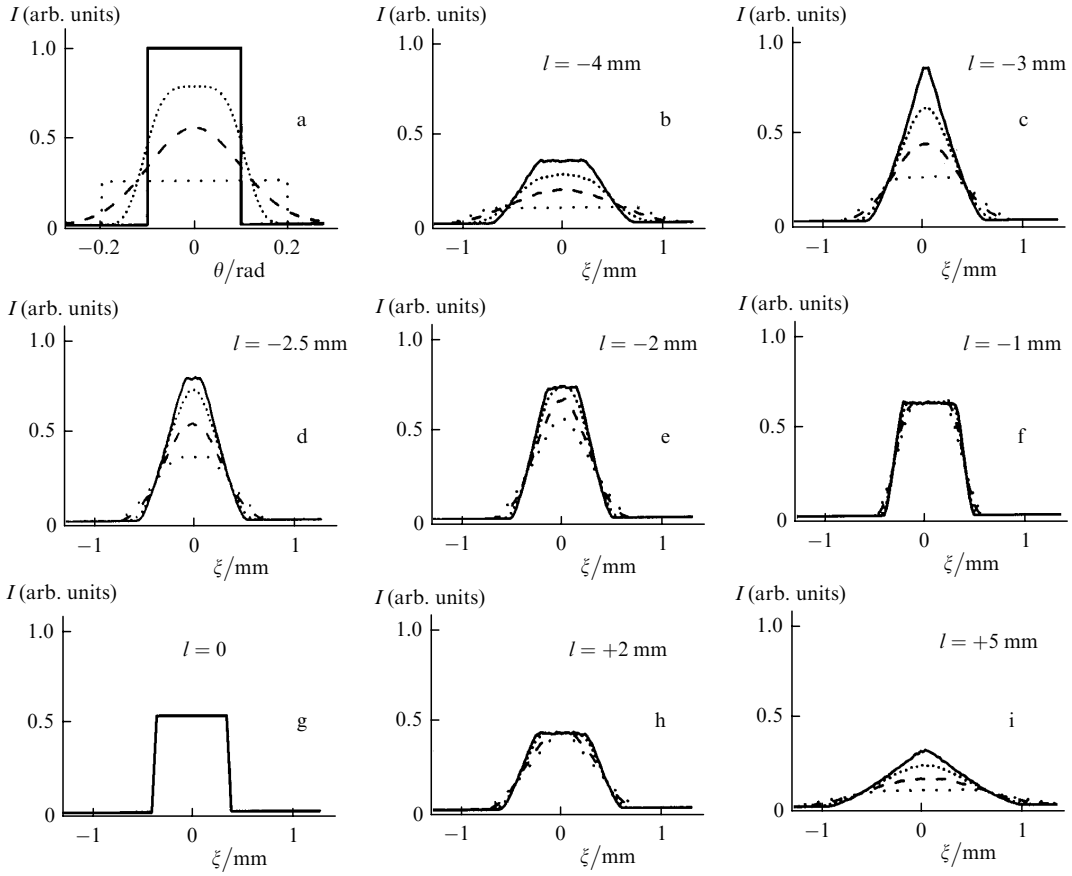


**Figure 4.** Intensity distributions (b–i) in the vicinity of the image plane for the uniform radiation distribution over the fibre end and different angular distributions (a) at the fibre output for different distances $l$ from the image plane.

distance exceeding 2 mm. An important result of the simulation is the presence of a region where the radiation intensity and, hence, the gain on the axis noticeably exceed the radiation intensity in the end image plane. This region is located between the focal region of the lens and the image plane. The transverse intensity distribution corresponding to the maximum radiation intensity on the axis has nearly triangle shape, which is most pronounced in the case of the rectangular angular radiation distribution at the fibre output (Fig. 4c).

The maximum radiation intensity on the axis is achieved approximately at the point where the beams emerging from the fibre edges are intersected. The broader the angular distribution, the closer this point to the end image plane. Correspondingly, the position of the plane in which the radiation intensity has a triangle distribution depends on the width of the angular distribution. The region size and the maximum radiation intensity are sensitive to the shape and width of the angular radiation distribution at the fibre output. Thus, as the fibre numerical aperture is increased from 0.1 to 0.2, the maximum radiation intensity on the axis considerably decreases. The transverse intensity distributions in this region favour the formation of a soft aperture due to a profiled gain. The transverse intensity distributions behind the image plane (Figs 4h, i) also lead to the formation of a soft aperture, but at a lower intensity and a weaker dependence of these distributions on the angular distribution at the fibre output. This is explained by the fact that in front of the image plane of the fibre end the image is transferred with reduction, while behind the image plane the image is transferred with magnification.

We verified our model by using a lens with a focal distance of 15 mm, which was corrected for spherical aberration and employed to transfer the fibre end image at the 1 : 1 scale. The spatial intensity distribution was recorded with a DeltaTech CCD camera ($1329 \times 1040$ pixels) with the dynamic range $\sim 10^3$. Figure 5 shows the intensity distributions recorded in the fibre end image region and the results of calculations performed with the Gaussian angular distribution, which is most close to the experimental angular distributions (see Fig. 2b). The calculated intensity distributions agree with the experimental distributions with accuracy sufficient for calculating the population inversion in active media.

In order to obtain the maximum lasing efficiency by preserving the acceptable quality of a mode, it is necessary to use the real population inversion distributions formed by a pump beam for different distances between the lens and the active element end. Our model takes into account the absorption, refraction and propagation of beams in the active element in the calculation of the inverse population, which becomes especially important with decreasing the

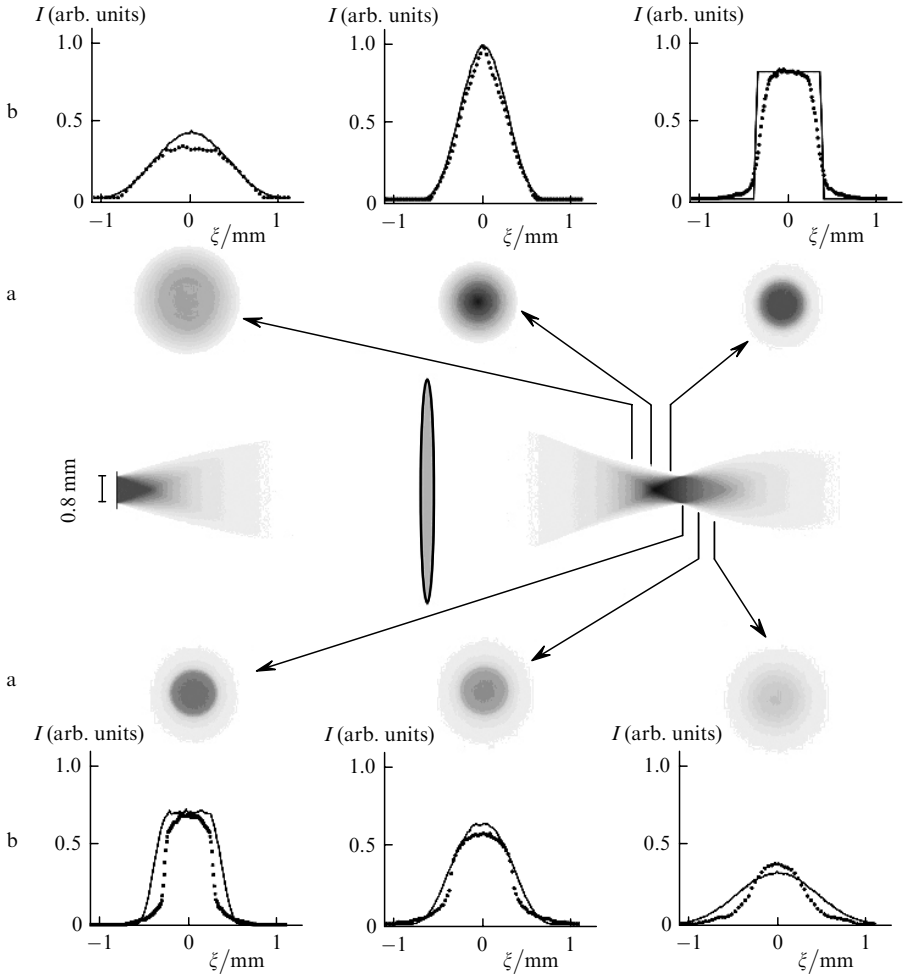


**Figure 5.** Experimental radiation intensity distributions (a) and profiles of calculated (solid curves) and measured (dashed curves) distributions (b) in different cross sections of the pump beam.

absorption coefficient. For Nd : YAG active elements (Nd concentration is 1 %), the maximum of the absorption coefficient ($\sim 10\ cm^{-1}$) is located at 0.808 μm. Upon detuning to 0.805 μm, the absorption coefficient decreases down to $\sim 4\ cm^{-1}$. As a rule, diode pumping of Nd : YAG active elements is performed at a wavelength of 0.808 μm. The length of a pumped region can be increased by changing temperature. The pump wavelength decreases by $\sim 4$ nm upon cooling the diode array by 10 °C. Figure 6 shows the inverse population distributions in the Nd : YAG active element obtained for different positions of its end in the pump beam and the absorption coefficients of 10 and $4\ cm^{-1}$. One can see that the inverse population distribution can be controlled by changing the diode array temperature.

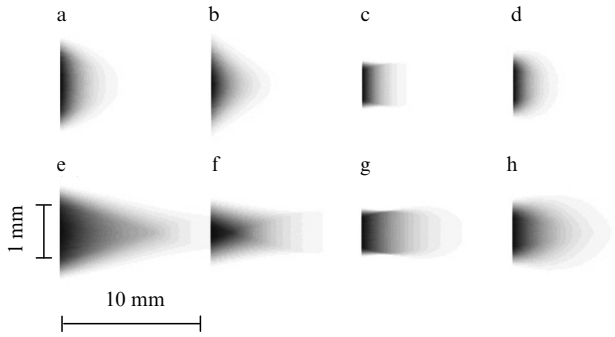


**Figure 6.** Inversion population distributions in an active element for the absorption coefficient of 10 (a–d) and $4\ cm^{-1}$ (e–h) and distances between a lens and the front face of the active element equal to 23 (a, e), 26 (b, f), 29 (c, g), and 32 mm (d, h).

Thus, the propagation of radiation from a diode array with a pigtail can be adequately described by using a simple model. We have calculated the radiation intensity distributions over cross sections for different angular distributions. There exists a region where the radiation intensity on the axis exceeds the intensity in the fibre end image plane. The maximum intensity on the axis is achieved when the transverse distribution of pump radiation is close to a triangle distribution.

The model proposed in the paper enables the calculation of the spatial distribution of the inverse population in the active medium upon longitudinal pumping by using the known spatially-angular radiation distribution at the fibre output. The inverse population distribution near the axis plays the role of an intracavity aperture. The rectangular inversion distribution acts as a rigid aperture. It is preferable to displace the front face of the active element from the image plane to the lens because this provides a higher gain and a passage to the soft-aperture regime. To obtain the maximum efficiency by preserving the acceptable mode quality, it is necessary to calculate the mode field as a function of the active-element position and variable parameters of the resonator by using the real spatial inversion distribution. Note that the gain saturation should be finally taken into account.

***Acknowledgements.*** The authors thank V.A. Bogatyrev, A.V. Vinogradov, and V.A. Petukhov for useful discussions. This work was partially supported by the Russian Foundation for Basic Research (Grant No. 05-02-17448a) and the program of the Division of Physical Sciences, RAS, 'Laser systems based on new active materials and optics of structured materials'.

## References

1. Zehetner J. *Opt. Commun.*, **117**, 273 (1995).
2. Fujikawaw S., Furuta K., Yasui K. *Opt. Lett.*, **26**, 602 (2001).
3. Minassian A., Thompson B., Damzen M.J. *Appl. Phys. B*, **76**, 341 (2003).
4. Agnesi A., Dell'Acqua S. *Appl. Phys. B*, **76**, 351 (2003).
5. Paschotta R., ffus der Au J., Sp'uhler G.J., Morier-Genoud F., Hovel R., Moser M., Erhard S., Korszewski M., Griesen A., Keller U. *Appl. Phys. B*, **70**, S25 (2000).
6. Gorbunkov M.V., Konyashkin A.V., Kostryukov P.V., Morozov V.B., Olenin A.N., Rusov V.A., Telegin L.S., Tunkin V.G., Shabalin Yu.V., Yakovlev D.V. *Kvantovaya Elektron.*, **35**, 2 (2005) [*Quantum Electron.*, **35**, 2 (2005).
7. Laporta P., Brussard M. *IEEE J. Quantum Electron.*, **27**, 2319 (1991).
8. Chen Y.F., Liao T.S., Kao C.F., Huang T.M., Lin K.H., Wang S.C. *IEEE J. Quantum Electron.*, **32**, 2010 (1996).
9. Sanches F., Chardon A. *Opt. Commun.*, **136**, 405 (1997).
10. Zhang X., Zhao S., Wang Q., Ozygus B., Weber H. *IEEE J. Quantum Electron.*, **35**, 1912 (1999).
11. Martel G., Labbe C., Sanches F., Fromager M., Ait-Ameur K. *Opt. Commun.*, **201**, 117 (2002).
12. Logunov O.A., Nikolaenko D.A., Startsev A.V., Stoilov Yu.Yu. *Kvantovaya Elektron.*, **19**, 231 (1992) [*Quantum Electron.*, **22**, 210 (1992)].